Polymer Characteristics and Fracture Morphology of Radiation-Polymerized Methyl Methacrylate-Impregnated Mortar

VIJAY K. BHATTACHARYA, MRINAL M. MAITI, and SUKUMAR MAITI, *Polymer Division, Materials Science Centre, Indian Institute of Technology, Kharagpur 721302, India*

Synopsis

Normal portland cement mortar–PMMA composites have been prepared under different doses of Co-60 gamma irradiation. The polymerization characteristics of MMA inside mortar and in bulk, mechanical and durability properties, and fracture morphology of the composites have been studied. The rate of *in situ* polymerization has been found to be faster than that in bulk. The molecular weights of the *in situ* and bulk PMMA were greatly reduced when a relatively higher dose of radiation was employed for the polymerization. However, the molecular weight of the PMMA-bulk was found to be higher than that of PMMA-in situ. The flexural/compressive strength and chemical durability in dil · H_2SO_4 medium of mortar–PMMA composites were, in general, superior to those of mortar–PS, though they declined under prolonged exposure to gamma irradiation. SEM micrographs of the fractured surface of the composites suggest a strong mortar–PMMA interfacial bonding and varied texture of the imbibed polymer in the matrix.

INTRODUCTION

Reported work on mortar–poly(methyl methacrylate) (PMMA) system mainly deals with strength and durability properties of the composites. However, some reports provide informations on the characteristics of *in situ* polymerization of MMA. Munoz-Escalona and Ramos have studied the rates of thermocatalytic[1] and gamma-ray-induced *in situ* polymerization.[2] Molecular weight of the impregnated PMMA has been determined by many workers.[1–5] In some of these reports[1–3] a higher rate of polymerization inside the mortar matrix than in bulk has been observed. At the same time the molecular weight of PMMA has been found to be higher in case of in-situ polymerization, which is, obviously, not in conformity with the general kinetics of free radical polymerization. Further, it is believed that the failure mechanism of polymer-impregnated concrete (PIC) is very much different from the one observed in normal concrete.[6] However, there have been very few attempts to study the fracture morphology of these composites and the distribution of polymer in the mortar matrix. In a previous publication[7] we reported polymerization characteristics in and fracture morphology of mortar–polystyrene (PS) composite. In this communication we report the results of our investigation of *in situ* and bulk polymerization of MMA, the fracture morphology of mortar–PMMA composite, and the effect of gamma irradiation on flexural, compressive strengths and durability properties of the composite.

Journal of Applied Polymer Science, Vol. 30, 1935–1947 (1985)
 CCC 0021-8995/85/051935-13$04.00

EXPERIMENTAL

Materials

Normal portland cement (ACC, India), sand (Cossey river bed) retained between sieves BS25 and BS52, and monomer (methyl methacrylate (MMA), Gujarat Chemicals, India), methyl ethyl ketone (BDH, India), methanol, and benzene (Sarabhai M. Chem., India) were used.

Specimen Preparation

Mortar specimens were prepared according to the specifications of ASTM 303-65 with sand/cement ratio of 3.0 and water/cement ratio 0.5. Prisms and cylinders of dimensions $10 \times 2 \times 2$ cm and 5×2.5 cm ϕ, respectively, were cast for flexural and compressive testing.[7]

Impregnation and Polymerization

Monomer impregnation was carried out by the method of Villamizar et al.[8] Dried mortar specimens were evacuated for 6 h to 2–4 mm Hg. Freshly distilled monomer (MMA) was introduced while maintaining the vacuum. The monomer did not contain any dissolved initiator, promoter, or catalyst.

In situ polymerization was carried out by gamma irradiation using a Co-60 source (Gamma Chamber 900 Unit, BARC, India). The intensity of radiation was found to be 0.1066 Mrad/h at the time of the experiments. Specimens were irradiated for a predetermined time. Residual monomer was removed by vacuum at 40°C. Percent monomer conversion, polymer loading, and monomer loss were determined gravimetrically.

Bulk polymerization of MMA was carried out in small penicillin ampoules under identical conditions.

Mechanical Properties

Flexural and compressive strength of MMA-impregnated, radiation-polymerized mortar samples [PIC(R)–PMMA] were determined with a Universal Testing Machine (Fu10,000e, Veb Thuringer Industrie Werk, East Germany) by center point and uniaxial loading, respectively.

Polymer Extraction and Molecular Weight

A weighed quantity of a ground PIC(R)–PMMA sample of BSS-100 mesh size was subjected to Soxhlet extraction for 72 h, using methyl ethyl ketone as the solvent. Extracted PMMA was precipitated by methanol, purified by reprecipitation, and finally dried under vacuum at 50°C to constant weight. This polymer is referred to hereinafter as PMMA-*in situ*. The values of percent extractable PMMA from the composite are average over three closest ones obtained from sets of five or six test specimens in each case.

PMMA samples prepared by bulk polymerization (PMMA-bulk) were also purified by the same procedure.

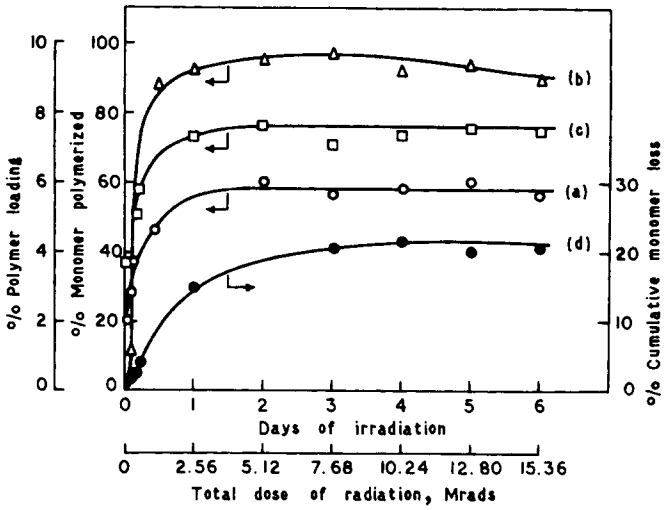

Fig. 1. Rate of conversion of MMA in *in situ* polymerization (a) and in bulk polymerization (b). Variation in percent polymer loading (c) and percent cumulative monomer loss (d) with days of irradiation.

Intrinsic viscosity of the polymers, PMMA-*in situ* and PMMA-bulk, was determined in benzene at 30 ± 0.1°C by an Ubbelohde suspended level viscometer. The viscosity average molecular weight ($\overline{M}_v$) was determined using equation[9]

$$[\eta] = 5.2 \times 10^{-5} \overline{M}_v^{0.76}$$

Durability

Durability of PIC(R)–PMMA samples in aqueous H_2SO_4 (5% w/w) solution was determined in terms of cumulative weight loss after 3, 7, 10, and 27 days of immersion in a stagnant environment. The acid solution was changed after 3, 7, and 10 days.

Fracture Morphology

Fracture surfaces of the PIC(R)–PMMA samples were cut after performing flexural tests and vacuum-coated with graphite followed by silver. Scanning electron micrographs (SEM) were taken in an ISI-60 Model within 48 h of mechanical testing.

RESULTS AND DISCUSSION

Polymerization Characteristics

In the case of *in situ* polymerization conversion of the monomer increases exponentially with days of irradiation and reaches a maximum of about

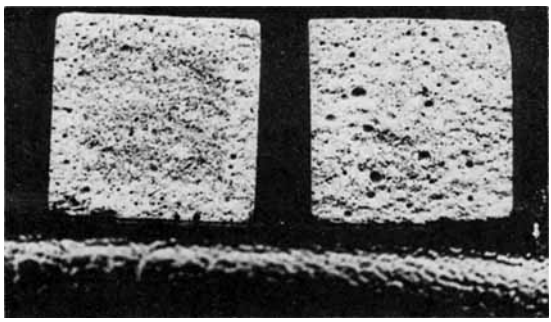

Fig. 2. Photograph of flexure fracture surfaces of an unimpregnated (right) and a PMMA-impregnated (left) mortar. The polymer free outer zone is created due to the evaporation of the monomer during irradiation.

60% around 2 days (~5 Mrad) of irradiation (Fig. 1, curve a). Similar results have also been reported by other workers.[10] A higher conversion could not be achieved due to loss of monomer by surface evaporation (Fig. 2). The monomer loss increases with the time of irradiation and reaches a maximum of 21% after 4 days (~10 Mrad) of irradiation under the experimental conditions (Fig. 1, curve d).

The maximum conversion (97%) in the bulk polymerization of MMA has, however, been obtained at about 3 days (~7.7 Mrad) of irradiation (Fig. 1, curve b). It is to be noted that, though the conversion is substantially lower in *in situ* polymerization compared to that in bulk polymerization, the maximum in the former is attained in 2 days compared to 3 days in the latter. These facts probably suggest a somewhat faster rate of polymerization of MMA inside the mortar matrix than in bulk. This is also supported by a shorter time (~4.5 h) required to reach a maximum in the molecular weight of PMMA in *in situ* polymerization than that in bulk (~6 h) (Fig. 3). Similar observations have also been reported during radiation polymerization of MMA with kaolin clay[11] and cement paste.[2] The faster rate of polymerization of MMA has been claimed to be due to the catalytic effect of the substrate matrix,[11] reduced gell effect,[3] and a possible energy transfer effect.[12]

So far as polymer loading in PIC(R)–PMMA composites is concerned, it also increases exponentially and attains a maximum (7.7%) at 2 days (~5 Mrad) of irradiation (Fig. 1, curve c).

Polymer Extraction

Polymer inside the cement–mortar matrix primarily acts as a pore filler.[13] However, a fraction of the impregnated polymer interacts with the substrate matrix and forms stable bonds. This chemically bound polymer has been termed as "inserted polymer" whereas the other fraction has been termed as "homopolymer."[11] It is possible to extract the homopolymer by Soxhlet extraction by using some suitable solvent. The inserted polymer will, however, keep adhering to the matrix and can be separated only by destroying

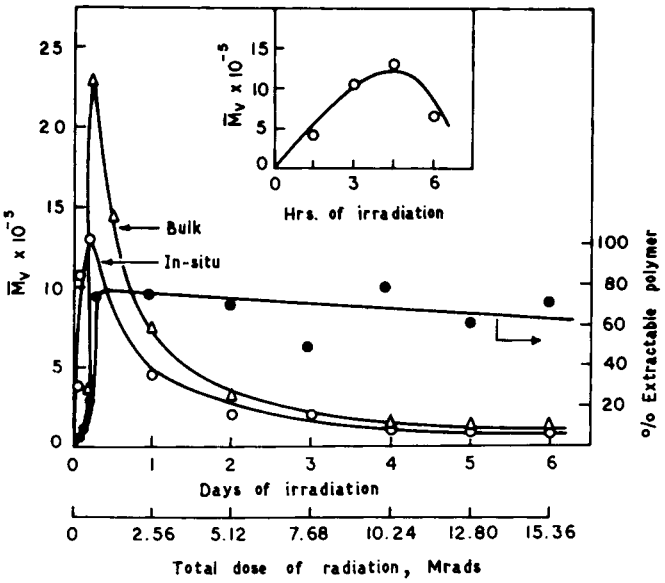

Fig. 3. Variation in percent extractable polymer; $\bar{M}_v$ of PMMA-*In situ* and PMMA-bulk with days of irradiation. The inset shows the variation in $\bar{M}_v$ of in situ PMMA at initial stages of irradiation in enlarged form.

the cement matrix with hydrofluoric acid[11] or saturated salicylic acid–methanol solution.[14]

The amount of extractable PMMA varies between 4% and 18% in case of the composites prepared by a relatively lower dose of radiation (0.16–0.48 Mrad). The amount increases substantially (48–78%) for the composites prepared with a total dose of 0.64 Mrad or more (Fig. 3). A definite trend is, however, observable between the total dose of radiation and the amount of extractable polymer.

Molecular Weight

The variation of the viscosity average molecular weight ($\bar{M}_v$) of PMMA-*in situ* and PMMA-bulk with dose of irradiation has been illustrated in Figure 3.

In both cases, $\bar{M}_v$ increases at initial stages of irradiation and after attaining a maximum value falls asymptotically to about 1×10^5. It is to be noted that, though the $\bar{M}_{v,max}$ in PMMA-*in situ* is much lower (13×10^5) than that in PMMA-bulk (23×10^5), the maximum in the former case is attained only in 4.5 h of irradiation compared to 6 h in latter case. This also suggests of a faster polymerization rate inside the mortar matrix. The observed difference in the trends of rate and molecular weight in bulk and *in situ* polymerized PMMA may be explained by production of higher concentration of initiating species inside the pores than in bulk.

It seems quite plausible that the initiation of polymerization would be much faster at the matrix–polymer interface whereas the propagation

would be limited in the bulk of the organic phase, thus decreasing the molecular weight. Higher thermal insulation offered by the mortar matrix may also help accumulation of the evolved heat of polymerization, resulting in an increased temperature and hence a faster rate of polymerization and lower molecular weight. The trends in rate and molecular weight in *in situ* polymerization compared to that in bulk may also be explained in terms of total radiation received by the monomer in unit time. The monomer is distributed over more space in the mortar matrix than in the bulk. Therefore, the same amount of monomer would receive more radiation in the mortar than in the bulk due to increased surface area, although the radiation intensity remains the same in both the cases. This would result in an increased number of propagation centers and, consequently, lower molecular weight of the polymer.

However, contrary to our observations on the rate and molecular weight, Munoz-Escalona and Ramos[2] report higher molecular weights of PMMA-*in situ* than that of the PMMA-bulk, when the polymerization was conducted with a total dose of 1.68 Mrad or more. In other publications[1,3] similar trends have been reported at all levels of temperature and initiator concentration when the polymerization is carried out thermocatalytically. Their observations appear to be not in keeping with the general kinetics of free radical polymerization.

The gradual decrease in the molecular weights of PMMA-*in situ* and PMMA-bulk with increasing total dose (Fig. 3) is a result of the degradation of the PMMA. The polymer is known to have very high susceptibility towards chain scission under the influence of gamma radiation.[15]

Mechanical Properties

Both the flexural and compressive strength of PIC(R)–PMMA are found to attain the maximum value at about 5 Mrad of irradiation and thereafter

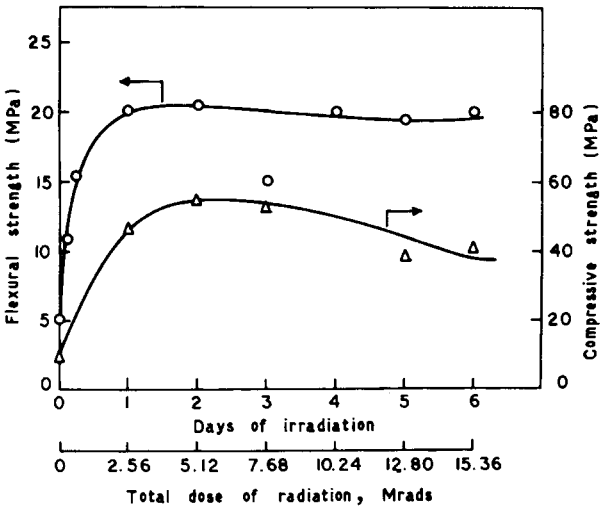

Fig. 4. Variation in flexural and compressive strengths of PIC(R)–PMMA composite with days of irradiation.

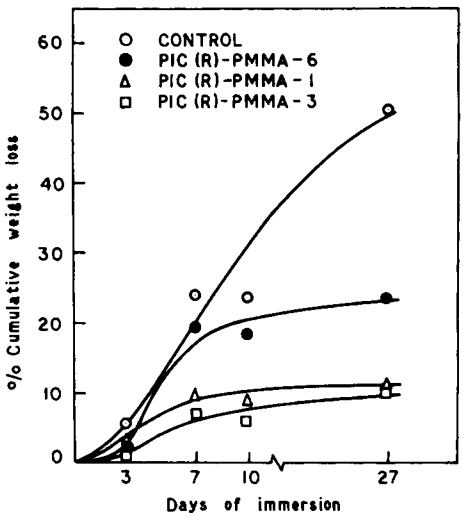

Fig. 5. Variation in percent cumulative weight loss of PIC(R)–PMMA composites in aqueous H_2SO_4 (5% w/w) with time, temperature-ambient, environment-stagnant: (○) control; (●) PIC(R)–PMMA-6; (△) PIC(R)–PMMA-1; (□) PIC(R)–PMMA-3.

declines very slowly, if at all (Fig. 4). This may be attributed to the gradual degradation of the impregnated PMMA upon prolonged exposure to gamma radiation. It may be mentioned here that styrene-impregnated mortar prepared at relatively higher radiation dose (~15 Mrad) exhibited higher flexural strengths.[7] This was explained on the basis of the fact that styrene, unlike MMA, had higher crosslinking to scission ratio under the influence of gamma irradiation.[7]

It is interesting to note that both the compressive and the flexural strength attain respective maxima where percent conversion to polymer in mortar matrix is also the maximum (Fig. 1, curve c). This points to the fact that the mechanical strength of mortar–polymer composites is dependent both on the percent polymer loading and molecular weight of the imbibed polymer in the PIC specimen.

Durability

It is apparent from Figure 5 that for all the composites the rate of weight loss is quite fast up to 7 days of immersion; beyond 7 days the rate becomes very slow.

The somewhat inferior durability of PIC(R)–PMMA-6 compared to PIC(R)–PMMA-1 and -3 may be due to the deliterious effect of prolonged exposure of gamma ray. The sharp drop in the molecular weight of PMMA-*in situ* (Fig. 3) under the influence of longer irradiation might have a bearing upon the poor durability of the composite.

In contrast to a gradual weight loss, all PIC(R)–PMMA composites, however, undergo considerable expansion in dimension in the test medium. A relative increase of the order of 10–15% in the diameter of the specimens has been observed after 27 days of immersion. However, PIC(R)–PMMA-6

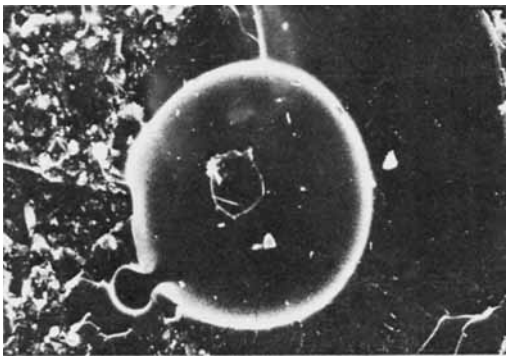

Fig. 6. SE fractograph of mortar–PMMA composite (× 120) cured at 3 days of irradiation, showing a thin film of the polymer adhered to the inner wall. Some well-defined hexagonal crystal, presumably of hydrated trisilicate is visible at the middle of the void.

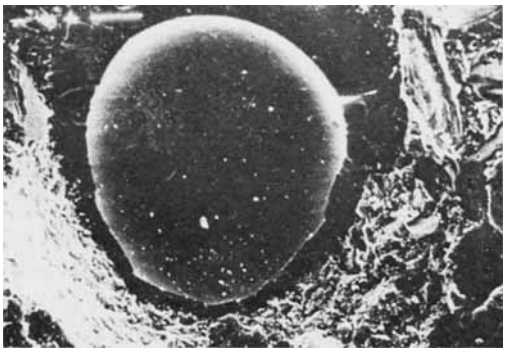

Fig. 7. SE fractograph (× 135) of a composite cured at 2 days of irradiation. A solid PMMA bead is clung to the inner wall of a macrovoid, possibly at the entry path of the monomer. The spherical shape of the bead and its attachment to the mortar matrix are unaffected even after flexural failure of the composite.

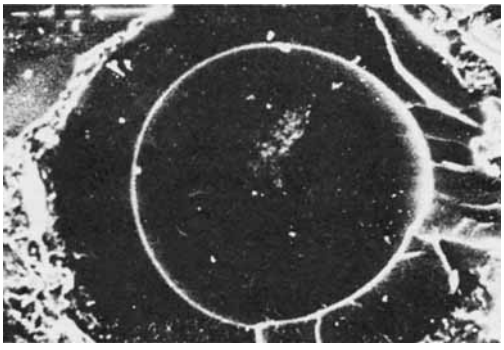

Fig. 8. Fractograph (× 87) of a mortar–PMMA composite cured at 5 days of irradiation. Cellular morphology of PMMA formed within a void is clearly visible. The fracture wave has propagated transversely without affecting the cell structure of PMMA.

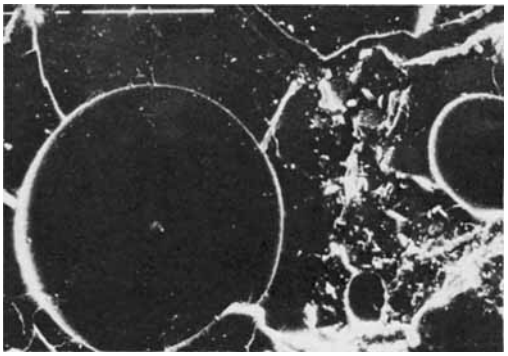

Fig. 9. PMMA foam (× 57) formed inside a macrovoid after 1 day of irradiation. A monomer entry path is visible at lower middle. A crack at upper right circumscribes the macrovoid. Yet the cell morphology of the imbibed PMMA and the boundary of the void in the form of a thin layer of the polymer remained unaffected, indicating a stronger mortar–PMMA interface.

registered rather a reduction in dimension at initial stages of immersion (3, 7, and 10 days). The control underwent reduction in size at all stages of immersion. Expansion of the PMMA-impregnated mortars in aqueous H_2SO_4 medium has been explained[16] on the basis of the fact that ester groups of PMMA undergo slow hydrolysis to give polymethacrylic acid (PMA) and methanol which are soluble in water. In the presence of strong acid such as H_2SO_4 the dissociation of PMA is suppressed, and it forms a swollen structure by absorbing water.[16]

In terms of durability in aqueous H_2SO_4 medium the PIC(R)–PMMA composites appear to perform better in comparison to their counterparts prepared by polystyrene [PIC(R)–PS]. For instance, PIC(R)–PMMA-6, which is the poorest in the PIC(R)–PMMA series, undergoes only 18.5% weight loss after 10 days of immersion (Fig. 5) whereas PIC(R)–PS-6 prepared and tested under identical conditions registered a weight loss of about 29%.[7] The better durability properties of PIC–PMMA composite than PIC–PS has been claimed to be due to the stronger PMMA–mortar interfacial bonding than PS–mortar.[16]

Fracture Morphology of PIC(R)–PMMA Composites

Scanning electron micrographs of the flexural fractured surface of PIC(R)–PMMA are significant for understanding the mechanism of composite failure, morphology, and ductility/brittleness of imbibed PMMA and, in particular, the mortar–PMMA interfacial adhesive strength.

Morphology of Imbibed PMMA. As will be evident from Figures 6–10, 13, and 14 the PMMA formed inside the mortar matrix is mainly present in the voids. The voids are never totally filled in unlike PIC(R)–PS composites.[7] This may be attributed to lower conversion (~ 60% max) of PMMA. This leaves behind a substantial amount of the volatile MMA which is removed by evacuation after irradiation for desired period of time. During escape of the unreacted MMA, PMMA retained in the voids assumes various

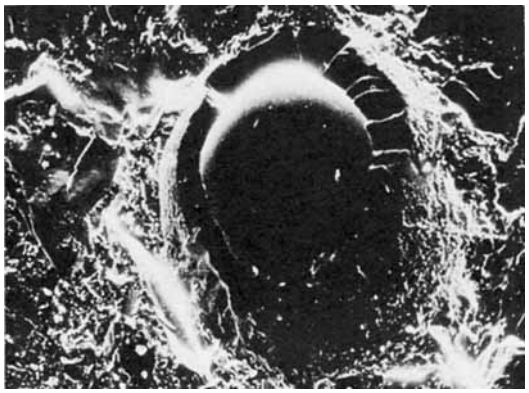

Fig. 10. A smoothly truncated but well-formed PMMA foam inside a void (× 86) after 2 days of irradiation characterized by a wide elliptical dimple at the center with a number of cell walls extending upto the void wall at the left, reminiscent of a strong interfacial adhesion between the mortar and the polymer. A monomer entry path is apparent at the lower right. Scattered deposits of PMMA around the void bear the impression of its ductility in the form of long fibrils, particularly at upper left and right.

texture and shapes. These may be simply a PMMA thin film adhering to the inner wall of the void (Figs. 6 and 14), a solid polymeric bead clung to the inner wall of the void (Fig. 7) possibly at the entry path of the monomer, cellular foams (Figs. 8–10) presumably formed by the evaporation of MMA from a highly viscous solution of low molecular weight PMMA in MMA, or a thick spherical PMMA shell (with well formed void inside) firmly attached to the inner wall of the void (Fig. 13).

Mortar–PMMA Interfacial Adhesion. The fractographs in Figures 7–10, 13, and 14 depict the fractured surface of PMMA contained in the mortar matrix. It is to be noted from the figures that no crack at the mortar–polymer interface could be traced and almost in every case the fracture surface represents a smooth plane on the polymer phase. These sharply contrast the characteristics of the polymer fracture surface in PIC(R)–PS composites,[7] where the fracture propagates along the weaker mortar–PS interface. This probably points to the fact that mortar–polymer (PMMA) interface is of higher strength compared to either that of the mortar or of the polymer. A close look at the nature of crack propagation in Figures 13 and 14 further corroborates the above fact.

Mechanism of Crack Propagation. It has been pointed out by several workers that the mortar matrix itself being a highly heterogeneous system provides certain inherent weak points from which the cracks start propagating when it is subjected to mechanical stress. Propagation of crack occurs along the path of least resistance. The micro or macro voids and the pore channel network are the weaker spaces, which are mainly responsible for faster crack propagation. Such conclusions are borne out by the fractographs presented in Figures 11 and 12.

In Figure 13, the crack has apparently moved from the mortar matrix through the imbibed PMMA in the void due to the fact that the two phases,

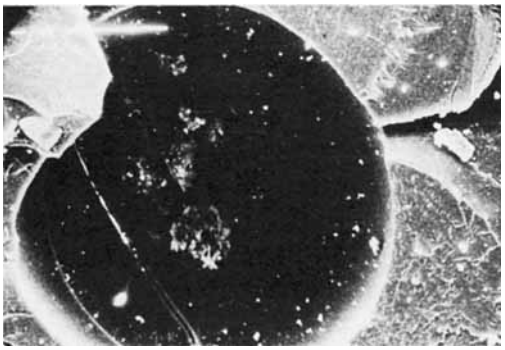

Fig. 11. The SE fractograph (× 100) of a composite cured by 10 days of irradiation. A macrovoid with no polymer inside. A wide crack, presumably formed during flexural failure of the composite, terminates at the void. Voids provide the path of minimum resistance to the crack propagation.

Fig. 12. Fine cracks generated around a sand particle during flexural testing of a composite obtained by 10 days of irradiation (× 90). The crack after branching has terminated to a microvoid at upper right.

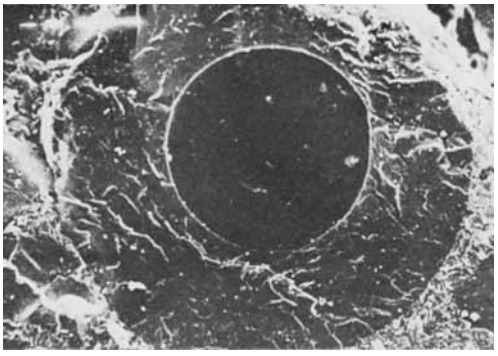

Fig. 13. Fractograph (× 107) of a mortar–PMMA composite cured at 6 days of irradiation shows a well-formed thick shell of PMMA inside a macrovoid. The mortar–polymer boundary is distinct. No impression of crack propagation along the interface is apparent, confirming a strong interfacial adhesion. The polymer fracture surface is typical of a brittle fracture, although some impressions of ductility, characterized by wavy flow patterns at upper right, are also apparent.

rather than the interface, provided the path of minimum resistance for fracture propagation.

Fracture Characteristics of Imbibed PMMA in the Mortar Matrix. Since the polymer inside the pores and voids of the cement matrix is present in a different texture, only a qualitative idea about its fracture pattern could be obtained from the SEM fractographs.

Figure 10 illustrates a transversely fractured cellular network of PMMA formed in a void after 2 days of irradiation. The scattered deposits of PMMA around the void bear impression of its ductile fracture in the form of long fibrils. The broken polymer shell (Fig. 14) obtained after exposure to 10 days of irradiation is typical of brittle fracture indicated by the absence of any flow marks of PMMA, although a substantial degradation of the polymer to lower molecular weight has taken place due to prolonged exposure to radiation.

At an intermediate exposure to radiation, i.e., 5 days, a ductile fracture of PMMA is quite apparent in Figure 15. The polymer is deposited at the periphery of a void (which, however, does not contain any polymer) with distinct flow marks. Figure 13, however, provides maximum details of the fracture surface of PMMA produced at 6 days of irradiation. The surface characteristics are basically of a brittle fracture (characterized by micropeaks); yet, some impressions of ductility are also apparent from the wavy flow patterns on the surface.

Mechanism of Reinforcement. Comparison of the strength properties of the PIC(R)–PS[7] and PIC(R)–PMMA composites, clearly indicates that impregnation of PMMA into mortar matrix offers a much higher degree of reinforcement compared to PS. Further, this enhanced reinforcement in PIC–PMMA is observed in spite of a lower loading of PMMA and much less compact texture of the same in the matrix compared to PS. These facts, however, indicate that the degree of void filling (or polymer loading) and the compactness (or texture) of the imbibed polymer are only of secondary importance in deciding the extent of reinforcement. Possibly the nature of the polymer, which solely determines the cement polymer interfacial adhesive strength, primarily determines the degree of reinforcement in PICs.

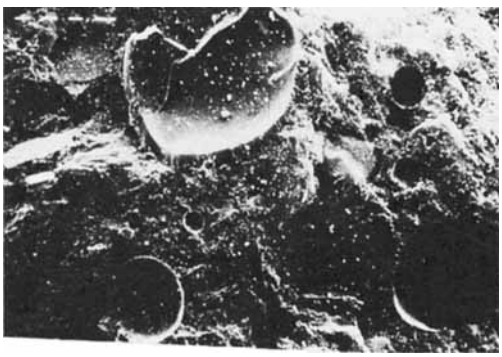

Fig. 14. Fractograph (× 123) of a mortar–PMMA composite cured at 10 days of irradiation showing a broken void (upper top) with a reasonably thick layer of PMMA firmly adhered to it, indicating a strong interfacial bonding between mortar and PMMA. The broken polymer shell bears the typical impression of a brittle fracture.

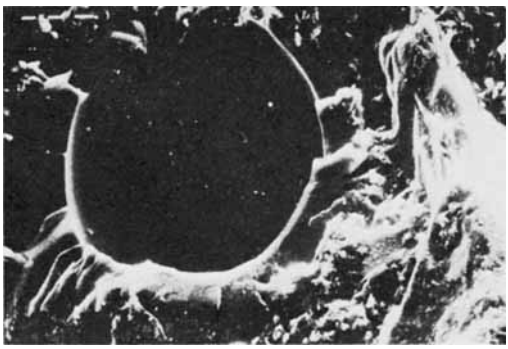

Fig. 15. A microvoid (× 152) in a composite cured at 5 days of irradiation. No polymer is formed within the void. Deposits of PMMA around the periphery of the void and at right correspond to the ductility of the polymer.

The authors wish to thank Department of Atomic Energy of the Government of India for financial assistance under Grant No.BRNS/Isotopes/26/78. Thanks are also due to Polymer Corp., Gujarat, and NOCIL, India, for a gift of MMA monomer.

References

1. A. Munoz-Escalona and C. Ramos, *J. Mat. Sci.*, **13**, 301 (1978).
2. A. Munoz-Escalona and C. Ramos, *Cement. Concr. Res.*, **6**, 273 (1976).
3. E. L. Madruga, J. San Roman, and J. Fontan, *Polym. Sci. Eng.*, **19**, 825 (1979).
4. K. Hastrup, F. Radjy, and L. Bach, in *Polymers in Concrete, Proceedings of the First International Congress on Polymers in Concrete,* Concrete Society, Lancaster, 1975, p. 43.
5. Y. Ohama, in Ref. 4, p. 60.
6. J. K. Bhargawa, *Polymers in Concrete,* Am. Concr. Inst., Detroit, 1973, pp. 205–221.
7. V. K. Bhattacharya, M. M. Maiti, B. Adhikari, and S. Maiti, *J. Appl. Polym. Sci.*, **29**, 2069 (1984).
8. C. A. Villamizar, A. Munoz-Escalona, and E. Duran, *J. Appl. Polym. Sci.*, **27**, 2151 (1982).
9. J. Bandrup and E. H. Immergut, Eds., *Polymer Handbook,* Wiley-Interscience, New York, 1966, Sec. IV, p. 26.
10. S. Ohgishi, H. Ono, K. Araki, and Y. Kasahara, in Proceedings of Third International Conference on Mechanical Behavior of Materials, Cambridge, England, August 20–24, 1979, Vol. 3, p. 3.
11. J. J. Beeson and K. G. Mayhan, *J. Appl. Polym. Sci.*, **16**, 2765 (1972).
12. M. Steinberg, L. E. Kukacka, P. Colombo, J. J. Kelsh, B. Manowitz, J. T. Dikeou, J. E. Backstorm, and S. Rubenstein, *Concrete-Polymer Materials, First Topical Report,* BNL 50134, Brookhaven National Laboratory, Upton, New York, 1968.
13. D. G. Manning and B. B. Hope, *Cem. Concr. Res.*, **1**, 631 (1971).
14. S. Takashina and F. Amano, in Review of the Thirteenth General Meeting of the Japan Cement Engineering Association, Tokyo, 1959, Paper 7.
15. A. R. Shultz, P. I. Roth, and G. B. Rathman, *J. Polym. Sci.*, **22**, 495 (1956).
16. V. K. Bhattacharya, K. R. Kirtania, M. M. Maiti, and S. Maiti, *Cem. Concr. Res.*, **13**, 287 (1983).

Received March 12, 1984
Accepted August 15, 1984